Astron. Astrophys. 320, 717–730 (1997)

ASTRONOMY
AND
ASTROPHYSICS

Evolution and dynamics of poor clusters of galaxies

Gastão B. Lima Neto⋆ **and Frank W. Baier**

Universität Potsdam, c/o Astrophysikalisches Institut Potsdam, An der Sternwarte 16, D-14882 Potsdam, Germany

Received 1 April 1996 / Accepted 7 October 1996

Abstract. We have performed N-body simulations of poor clusters with enough particles to resolve the individual galaxies. The main cases of initial conditions are: (i) 50 equal mass galaxies; (ii) 60 galaxies with masses drawn from a Schechter distribution function, and (iii) the collision of two subclusters each one containing 25 galaxies. The evolution and kinematics of the first ranked galaxy, the substructures, and the possible rotation of clusters are investigated.

A massive object with cD characteristics is always formed and is never found farther than 100 kpc from the centre of the cluster. This massive galaxy oscillates around the cluster centre with an average peculiar velocity of 70 km s^{-1}. We show that increasing the initial intra-cluster medium (ICM) mass while keeping the galaxies mass and structure without change, raises the merging rate due to the dynamical friction with the ICM. Substructures are almost always present on the galaxy count contour plots. The ICM projected density, which should be similar to the X-ray emission map, presents strong substructures when we have colliding subclusters. Otherwise, in isolated clusters, the substructure is less pronounced indicating that substructures should reflect important but transient dynamical phenomena. We propose that clusters formed by an off-centre collision and subsequent merging of two approximate equal mass subclusters should show a general rotational pattern that could be detected even after the relaxation of the cluster. These clusters would have a spin parameter, λ, of about 0.3–0.5.

Key words: galaxies: clusters of; formation; elliptical and lenticular, cD – galaxies: dynamics – methods: numerical – X-rays: galaxies

1. Introduction

Poor clusters of galaxies are important bound gravitational structures with velocity dispersion of 300–600 km s^{-1}, that are intermediate between groups (a few tens of galaxies) and rich clusters (many hundreds of galaxies). Poor clusters were first catalogued by Morgan et al. (1975) and Albert et al. (1977), and were shown to have optical and X-ray properties that are a smooth continuation of the characteristics of rich clusters of galaxies (Bahcall 1980). Recent studies (e.g. Dell'Antonio et al. 1995) have shown that the galaxy distribution in poor clusters reflects the X-ray distribution. Moreover, the mass in galaxies is about 5–10 % of the total mass and about half the gas mass.

As aggregates of galaxies, poor clusters provide some ideal conditions for the study of galaxies in 'community'. Given their velocity dispersion it is natural to expect that galactic interactions play a influential rôle in the galaxy and cluster evolution. Indeed, many poor clusters have a cD galaxy near its centre, that can be defined either by the galaxy distribution or the X-ray emission. There are two main theories for the formation of cD galaxies in clusters. First, they may be the result of a cooling flow of the intra-cluster gas at a rate of some tens of solar masses per year that piles up at the bottom of the cluster potential wells (e.g. Fabien et al. 1984). The second possibility is the formation by galactic cannibalism (Ostriker & Tremaine 1975) which is expected when phenomena like dynamical friction, tidal stripping, and mergers are common. Galactic cannibalism is often supported by the observation that at least half the observed cD galaxies have more than one nucleus, and the fact that the formation of central giant galaxies is easily obtained in N-body simulations of groups and clusters (e.g. Barnes 1988, Bode et al. 1994). Moreover, the extended envelope around cD galaxies can be explained by the accumulation of tidally stripped matter from galaxies at the bottom of the cluster potential wells (Merritt 1983).

Thus, although poor clusters in itself are important structures that bridges the well studied rich clusters and groups of galaxies, they may be also important if they are considered as the building blocks of rich clusters. Indeed, it is well known that many rich clusters have clear signs of substructures. The frequency and intensity of this subclustering, however, are a subject of debate. For instance, Baier et al. (1996) advocate that almost all clusters show clear substructures in the galaxy and X-ray distributions. On the other hand, Jones & Forman (1990) estimate that the fraction of clusters with double or multiple maxima in the X-ray distribution is 30%, Geller & Beers (1982) found about 40% of clusters having multiple peaks in the galaxy distribution, and the analysis of gravitational lens can suggest that the total

Send offprint requests to: G.B. Lima Neto

⋆ Present address: Observatoire de Lyon, France

mass distribution (i.e. including the invisible matter) may have substructures (Fort & Mellier 1994).

The systematic presence of multiple peaks in the distribution of the various components of clusters may be understood if clusters are formed by the merger of smaller units, that is, poor clusters of galaxies (McGlynn & Fabian 1984). Zabluboff and Zaritsky (1995) presented X-ray and optical evidence that the two substructures (separated by about 0.7 Mpc in the plane of the sky, with line-of-sight relative velocity of about 100 km s^{-1}) in the cluster Abell 754 are in the process of colliding. The cluster Abell 569 seems also to be formed by two subclusters that may be falling in a spiral towards each other (Beers et al. 1991, Baier et al. 1996). Finally, Ulmer et al. (1992) show that the centers of the X-ray and galaxies distributions of Abell 168 are probably disjoint. They interpret this as an evidence that this cluster was formed by a collision of two equal sized subclusters.

It is not clear however how these mergers of poor clusters may affect the intra-cluster medium (X-ray emitting gas and dark matter), the galaxies, and their relationship. Besides the dynamical process that operates in isolated virialized clusters like dynamical friction, two-body relaxation, tidal effects, and mergers of galaxies, there are also the effects due to encounters of clusters. Namely, we have the shock and eventual heating of the X-ray emitting gas, and the temporal variation of the total gravitational potential, leading to a violent relaxation of all components of the cluster. Another important point to consider is the possibility that the collisions of subclusters may not always be head-on but parabolic. In this case, and if the subclusters merge within a Hubble time, the final cluster may present a global angular momentum that may be determined observing the radial velocity of the galaxies.

Although theoretical models can describe fairly well and uncover the basic physics of 'well behaved' clusters – i.e. objects close to virial equilibrium, without strong substructure – (e.g. Merritt 1983), one needs numerical methods to follow in a self-consistent way the non-linear evolution of galaxies in clusters.

The present study addresses the dynamical evolution of isolated poor clusters as well as the collision of two clusters. In this work we will concentrate on the evolution of the first ranked galaxy of poor clusters, its formation and kinematics near the centre of the cluster; the evolution of the Mass (Luminosity) Function of the galaxies; and the presence of eventual substructures that may appear during the evolution.

Our main tool in this research is the use of self-consistent N-body simulations. This technique enables us to follow the time evolution from a given set of initial conditions to the present configuration. Our aim is to investigate different phases of the evolution of poor clusters of galaxies, including the encounters of subclusters, searching evidence for interactions among galaxies that occurred in the past and that may be responsible for the features observed today.

This paper is organized as follows: in Sect. 2 we describe the techniques employed and the initial conditions that defines our models. In Sect. 3 we describe our results concerning the formation of the first ranked galaxy (FRG), the presence of substructures (in the galaxy and the total mass distribution). In Sect. 4 we discuss our results in connection to previous theoretical and observational studies and we conclude in Sect. 5.

2. Method

2.1. Technique

We have used N-body simulations in order to study the evolution of galaxies in clusters. The equations on motion are integrated with the Tree-Code developed by Barnes & Hut (1986) and ported to FORTRAN and vectorized by Hernquist (1988). The Tree-Code is particularly well adapted for the simulations of granular systems (such as a cluster of galaxies), without imposing any geometric symmetry since it is of lagrangian type (i.e. gridless). We have used a time step of 0.25 time-units,[1] tolerance parameter of 0.75, and quadrupole correction. The softening parameter of each particle is equal to 0.5 length-units (or kpc, with our adopted scaling), a compromise value between obtaining runs with good energy conservation and the resolution need to well resolve the core of galaxies. With these parameters, the energy conservation is about 1% for 8400 time steps (corresponding to 13.3×10^9 years) using 46 000 equal mass particles.

In all runs the masses of the individual particles are the same in order to avoid spurious mass segregation (heavier particles falling towards the centre) due to two body relaxation.

2.2. Initial conditions

In order to follow the evolution of galaxies in clusters, we have used three main families of initial conditions in our simulations:

a) Isolated clusters with equal mass galaxies, without ICM.
b) Isolated clusters with galaxies following a Schechter (1976) luminosity function, with ICM.
c) Collision of two equal mass clusters of galaxies, with ICM.

Notice that ICM here means a dark intra-cluster medium of *collisionless particles*, not the intra-cluster dissipative X-ray emitting gas. When it applies (families b and c), an ICM is superimposed to the initial galaxy distribution. The function of the ICM is to mimic an assumed invisible matter component.

The initial conditions of our simulations should be regarded as the epoch between the relaxation of the cluster just after detaching from the Hubble flow and before appreciable interactions have affect the galaxies or the cluster itself. In all cases, the simulations are started with the clusters already relaxed, close to a virial quasi-equilibrium state.

The distribution of galaxies in rich clusters is usually well fitted by the isothermal King profile, which is often approximated by the analytic King profile (eg. Sarazin 1988, and references therein). Since poor clusters seems to be a physical continuation of rich clusters of galaxies (Bahcall 1980), one would expect that

[1] The units used to express the results of the simulations are scaled as (G = 1): [length] = 1.0 kpc, [time] = 6.325×10^6 yrs, [mass] = 5.56×10^9 $M_\odot$, [velocity] = 154.6 km/s, [μ] = 5.56×10^3 $M_\odot/\mathrm{pc}^2$ and [ρ] = 5.56 $M_\odot/\mathrm{pc}^3$.

Table 1. Initial conditions of the Plummer galaxy used as a clone. The dynamical time scale, $t_{\rm dyn}$ is defined as $GM^{5/2}/2|E_{\rm tot}|^{3/2}$ and $r_{\rm c}$ is the core radius

No points	500	$M_{\rm tot}$	90
$r_{\rm c}$	20	Total Energy/$M_{\rm tot}$	-1.27
$t_{\rm dyn}$	31.6	$2E_{\rm cin}/\|E_{\rm pot}\|$	0.095

the King profile would also apply for poor clusters. However, due to small number statistics, in practice it is difficult to determine precisely the galaxy distribution in poor clusters. In any case, the analytic King profile is just an approximation of the true King distribution, the main difference between them being the asymptotic behaviour. The true King distribution has a finite mass and extent, while the analytical one is infinite.

For this reason we chose to use a Plummer distribution (which is fully analytical) in order to model the initial conditions of our simulated clusters. The Plummer profile has a finite mass and is very close to the analytical King profile for $r \lesssim 10 r_{\rm c}$ (taking into account that the core radius, $r_{\rm c}$, of a Plummer sphere should be about 1.75 times greater than the corresponding King core radius).

Below, we give the details of the construction of each family of initial condition.

2.2.1. Clusters with equal mass galaxies

In this case, each member of the cluster is a clone of a galaxy that is modelled according to the following 'recipe'. The particles that make up the galaxy are placed randomly in a Plummer sphere of total mass $M_{\rm tot}$,

$$\rho(r) = \frac{3}{4\pi}\frac{M_{\rm tot}}{r_{\rm c}^3}\left[1+\left(\frac{r}{r_{\rm c}}\right)^2\right]^{-5/2}, \quad (1)$$

having a very low velocity dispersion, so that the total potential energy is much greater than the total kinetic energy. Table 1 summarizes its properties.

After generating the Plummer sphere, we followed its evolution in isolation with the Tree-Code for 800 time-units, about 25 $t_{\rm dyn}$. Since the object is initially cold ($2E_{\rm cin}/|E_{\rm pot}| \ll 1$) it collapses on a time scale of $\sim 1/\sqrt{G\overline{\rho}}$, about the order of its dynamical time scale. After the collapse, the sphere oscillates a few times, and relaxes to a quasi-equilibrium virial configuration. This dissipationless collapse results thus in a relaxed object structurally similar to an elliptical galaxy. The half-mass radius decreases to 13.3, about half the initial value 26.1 ($1.305 \times r_{\rm c}$, for a Plummer sphere). The projected density profile is well fitted by a de Vaucouleurs law.

The clusters of equal mass galaxies are then created by placing clones of this 'elliptical galaxy' on another Plummer sphere, now representing the cluster. Now, however, the velocity dispersion of the particles (which represent the galaxies in the cluster) is chosen so as that the cluster is in virial equilibrium. The velocity of each galaxy is drawn randomly from a isotropic maxwellian distribution. Notice that initially all mass is in the galaxies.

Table 2. Properties of the clusters having equal mass galaxies. $r_{\rm coup}$ is the initial radius of the cluster, $t_{\rm dyn}$ is the dynamical time scale, ℓ is the initial mean harmonic separation of the galaxies, and σ is the initial velocity dispersion.

Run Id	$r_{\rm coup}$	$t_{\rm dyn}$	ℓ	σ
AM1	1500	304	571	1.88
AM2	"	443	727	1.64

For each clusters the number of particles is 25 000, the total mass is 4500, and the core radius is 450.

We have done 2 simulations each one with 50 identical galaxies. Both simulations use the same set of structural parameters (Table 2) except that the seed of the random number generator was changed thus changing the actual distribution in the phase space (positions and velocities of the galaxies). Random fluctuations explain the differences on quantities like the total energy and the velocity dispersion between the two clusters.

The snapshots of the initial conditions and evolution of the cluster AM1 is shown as an example in Fig. 1.

2.2.2. Clusters with mass (luminosity) function

Contrary to the previous case, here the galaxies are generated already in a virial quasi-equilibrium state. The first step however is determining the masses of the individual objects before actually generating them. The masses of the galaxies were randomly drawn from a Schechter luminosity function

$$\phi(M) = \frac{\phi_*}{M_*}\left(\frac{M}{M_*}\right)^{\alpha}\exp(-M/M_*), \quad (2)$$

with the following parameters: $M_* = 40$, $\alpha = -1.1$. We also defined the mass range of the cluster as $M_{\rm min} = 8$ and $M_{\rm max} = 100$. Notice that this range implies a magnitude difference (assuming constant mass to luminosity ratio) of about 2.7 between the largest and smallest galaxies.

Having the masses, we generate virialized Plummer spheres scaling each object with $r_{\rm core} \propto M^{1/3}$ and making sure that all particles in the galaxy are gravitationally bound.

Like in the previous case, 60 galaxies were placed randomly in a Plummer sphere (now the cluster). A dark collisionless ICM is superimposed on the cluster. The ICM follows also a Plummer density profile and has the same core radius as the galaxy distribution. The fraction of mass in the ICM is reported in Table 3. The masses of the ICM particles are the same of the galaxies particles in order to avoid spurious segregation. The galaxy and ICM velocity dispersion were so that the clusters were initially in virial equilibrium. Since the ICM particles are initially in equilibrium with the cluster gravitational wells, they are not bound to the galaxies individually. Table 3 describes the initial conditions that we have used.

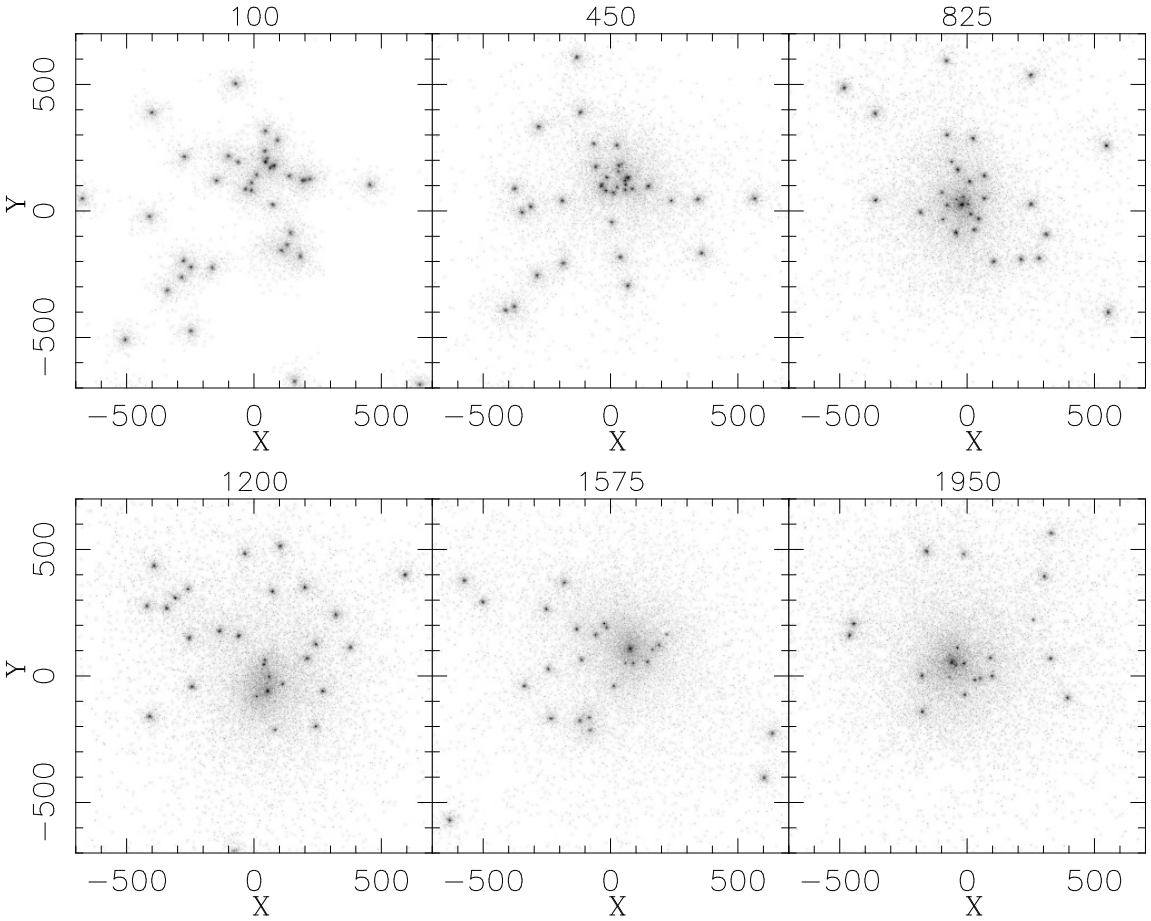

Fig. 1. The snapshots of the initial conditions and the evolution of the simulation AM1 (initially equal mass galaxies and no dark ICM). On top of each panel is the time. Note that an inter-cluster medium is created due to the stripping of mass from the galaxies, thus forming an envelope around the FRG

The snapshots of the initial conditions and evolution of the cluster AM4 is shown as an example in Fig. 2, where only the visible particles are shown.

2.2.3. Collision of equal mass clusters of galaxies

For this kind of simulation, we have put two subclusters (or substructures) in a collision trajectory. Each subcluster was created already in virial equilibrium as explained in the above paragraph. In this case, each subcluster contains 25 galaxies with masses sampled from a Schechter Function. The properties of the subcluster are given in Table 4.

The subclusters are put on a collision trajectory. We have simulated a head-on and three tangential collisions where the subclusters were in an initial elliptical orbit. A summary of the initial collision parameters is given in Table 5. In runs MS1, MS2 and MS3 we use the subclusters SA1 and SA2 with a total of 46 000 particles. In the MS4 simulation we use the pair SB1 and SB2 with a total of 70 000 particles.

The MS1 simulation is a head-on collision of two clusters while MS2, MS3 and MS4 are tangential collisions. The snapshots of the initial conditions and the evolution of the simulation MS3 is shown as an example in Fig. 3.

2.3. Counting and weighting the galaxies

Once we run a simulation we must keep track of the galaxies. This is not trivial for two reasons: the galaxies merge and they have their mass partially stripped by tidal encounters.

In order to determine in our simulations which particles belong to a given galaxy, and thus identify each galaxy at a given moment, we have used a percolation technique, the so-called 'friends-of-friends' algorithm (ex. Chincarini et al. 1988). This method is well adapted to localize the galaxies since it is independent of their shape or position inside the cluster. Another advantage of this method is that it selects objects having approximately the same overdensity at the border compared to the global mean density (West et al. 1988).

Briefly, in the standard percolation algorithm we define a sphere of radius $r_{\rm p}$ around each particle. The groups of particles with intersecting spheres are then identified as a 'candidate galaxy' in our simulations. From the group of particles making this 'candidate galaxy', we rejected those that have a velocity four times greater than the velocity dispersion of the group. In this way, we eliminated possible unbound particles. Finally, in order to avoid small groups of particles being identified as a galaxy, we have only accepted as a galaxy objects with a number

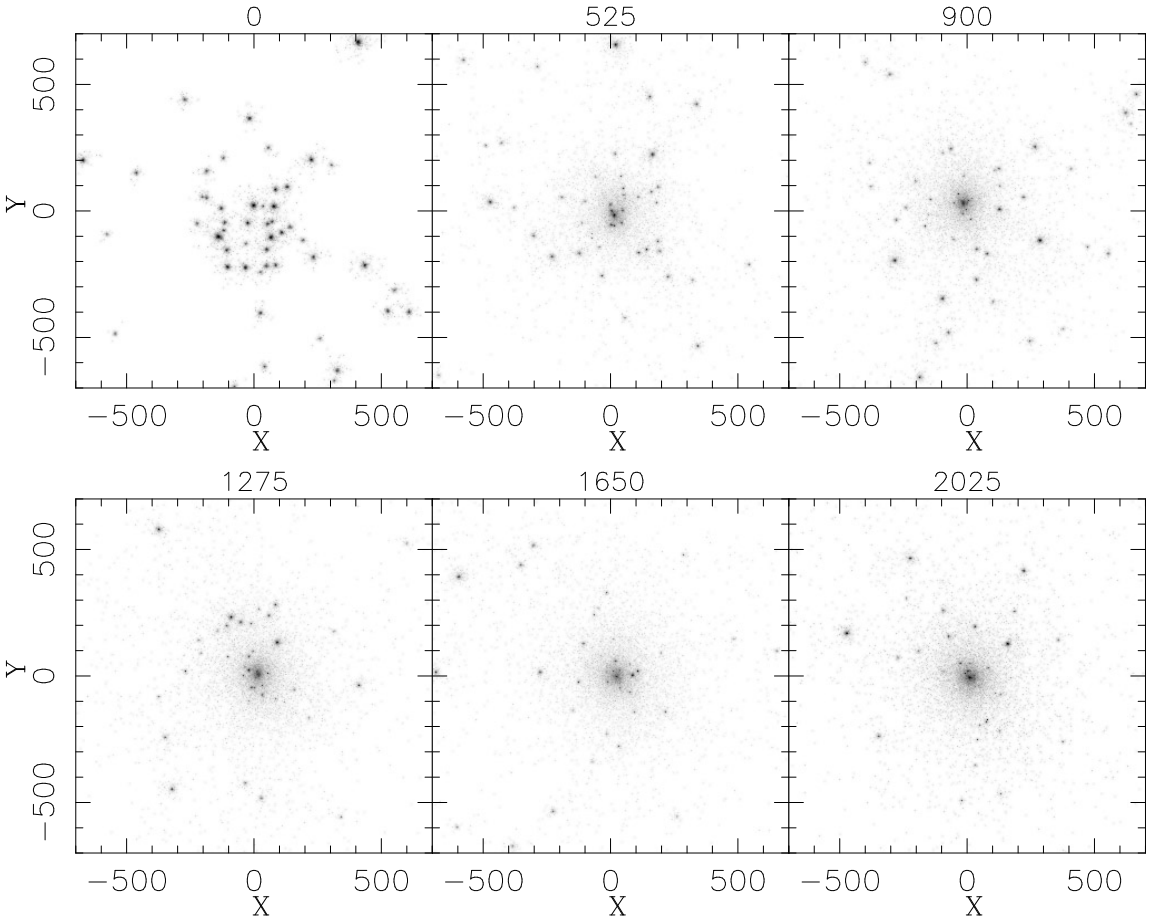

Fig. 2. The snapshots of the initial conditions and the evolution of the simulation AM4 (initially galaxies following a Schechter mass distribution and 0.67% of the total mass in the form of ICM). On top of each panel is the time. For clarity, the dark ICM particles are not plotted (but notice that a diffuse extra galactic component is formed due to the stripping of particles from the galaxies)

of particles above a given cut-off. This number depends slightly on the simulation being between 45 to 60 particles (we take into account only the visible particles, not the particles that forms the dark ICM).

There in no straightforward way to determine a priori the value of $r_{\rm p}$. Using a too small value we identify any concentration of particles as a galaxy; with a $r_{\rm p}$ too large, we cannot resolve galaxies that are close together. We tried different percolation radii and retained $r_{\rm p}$ = 4.5 for all runs. The objects thus found are in fact the cores of the galaxies since otherwise it would not be possible to distinguish between close galaxies.

Table 3. Properties of the cluster having galaxies that follow a mass function. ICM is the ratio of the ICM mass to the total mass of the cluster, $r_{\rm coup}$ is the initial cut-off radius of the cluster, $t_{\rm dyn}$ is the dynamical time scale of the galaxies, ℓ is the mean harmonic radius, and σ is the velocity dispersion.

Run Id	Mass	ICM	$r_{\rm coup}$	$t_{\rm dyn}$	ℓ	σ
AM3	2208	0.40	1200	433	249	1.27
AM4	4423	0.67	"	320	270	1.44
AM5	5519	0.67	"	400	252	1.35

For each run the number of particles is 45 000 and the initial core radius (Plummer model) is 150.

3. Results

3.1. Merging and the first ranked galaxy

In all simulations we observe the formation of a central giant galaxy by merging, which we will refer as the first ranked galaxy (FRG).

For the 2 simulations AM1 and AM2 (no ICM, starting with equal mass galaxies) the merging of galaxies starts at about one $t_{\rm dyn}$ and proceeds steadily until the end of the simulation (Fig. 4a). In the AM1 run, the FRG forms near the centre at about $2t_{\rm dyn}$, and it is well distinct from the remaining galaxies at $2.5t_{\rm dyn}$. This object will remain at or very near the centre of the cluster and will slowly cannibalize the other galaxies. We can still count 29 galaxies at the end of the simulation ($t \approx 12.8 \times 10^9$ years). The AM2 simulation, which is intrinsically similar to the AM1 (cf. Sect. 2.2.1) does *not* form a giant galaxy near the centre as quickly as in simulation AM1. An important

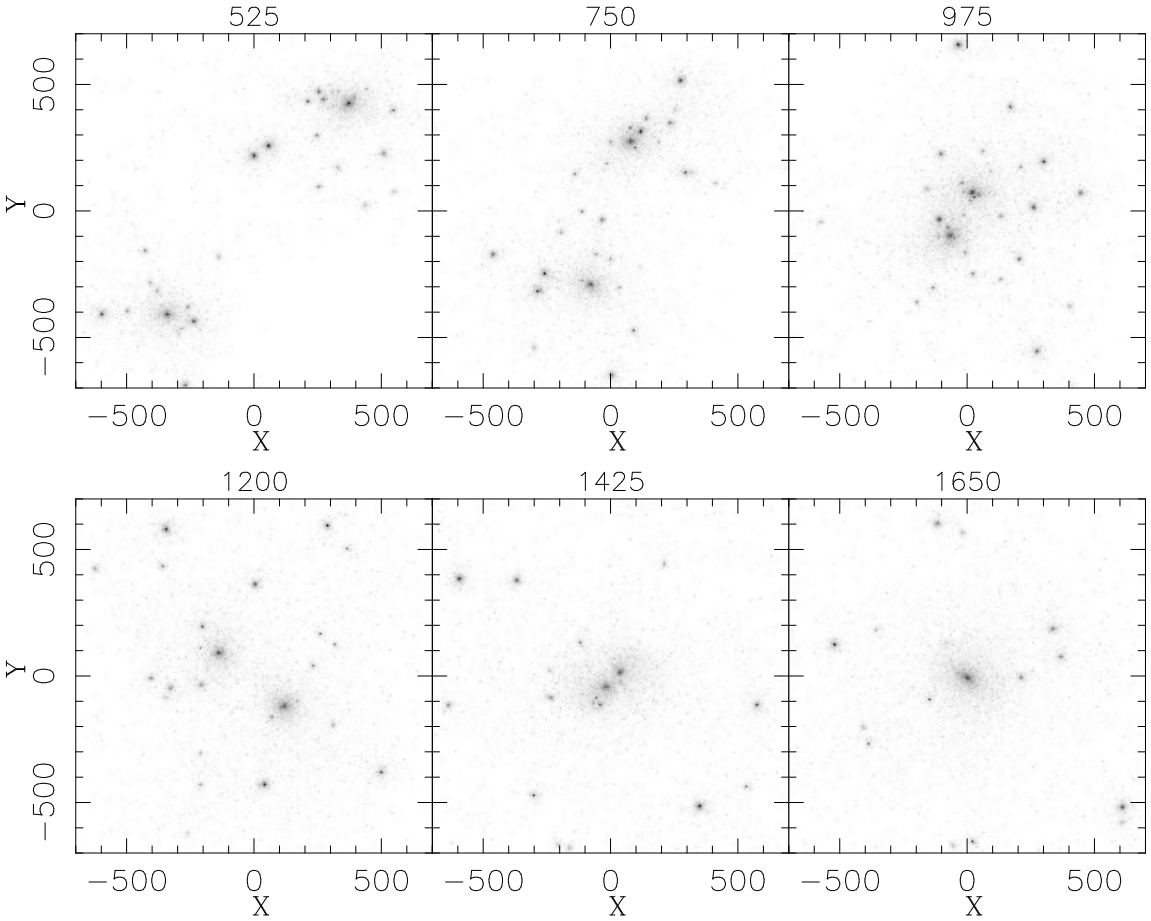

Fig. 3. The snapshots of the evolution of the simulation MS3 (collision of two clusters of 25 galaxies each with the galaxies following a Schechter mass distribution and 0.67% of the total mass in the form of ICM). On top of each panel is the time. As in Fig. 2, the dark ICM particles are not plotted

Table 4. Properties of the subclusters. M_* and $\alpha_{\rm Sch}$ are the parameters of the Schechter distribution. $M_{\rm gal}$ and $M_{\rm tot}$ are the masses in the galaxies and in the whole system, respectively. $t_{\rm dyn}$ is the dynamical time scale, σ is the velocity dispersion, and ℓ is the mean harmonic separation of the galaxies

Models:	SA1	SA2	SB1	SB2
Npts	23 000	23 000	35 000	35 000
$M_{\rm gal}$	623	602	602	623
$M_{\rm tot}$	1869	1805	1807	1871
$t_{\rm dyn}$	450	400	300	550
σ	0.91	0.93	1.05	0.81
ℓ	301	241	218	224

For the above models it we set $\alpha_{\rm Sch} = -1.1$, $M_* = 40.0$, ICM=67%, $r_{\rm core} = 100.0$.

Table 5. Properties of the systems of two colliding substructures. 'Sep.' is the initial separation between the centre of both substructures, $v_{\rm rel}$ is their relative velocity, ϵ and $T_{\rm orb}$ are the ellipticity and orbital period (oscillation for MS1) of the initial keplerian orbit. E/M and L/M are the total energy and angular momentum per mass unit

Run Id	Sep.	$v_{\rm rel}$	ϵ	$T_{\rm orb}$	E/M	L/M
MS1	2500	1.5	1.00	40400	−0.086	0.0
MS2	2500	1.5	0.86	40400	−0.086	562.5
MS3	1836	1.4	0.87	7910	−0.255	315.0
MS4	1836	1.4	0.87	7895	−0.256	315.0

FRG will only form after over than $3t_{\rm dyn}$ and it will only be in the centre of the cluster at about $4t_{\rm dyn}$ (see also Sec. 3.2).

The case of the three simulations AM3, AM4 and AM5 (with ICM, and the masses of the galaxies following the same Schechter distribution function) is different from the precedent. Here, there are already a few galaxies which are naturally (thanks to the mass distribution function) more massive than the average galaxy at the beginning of the run. These more massive galaxies fall faster than the others to the centre of the cluster, where they start to cannibalize the smaller ones. Thus, a central dominant galaxy quickly forms on these three simulations, independently on the amount of the ICM. However, the merging rate is strongly superior in the more massive cluster (more mas-

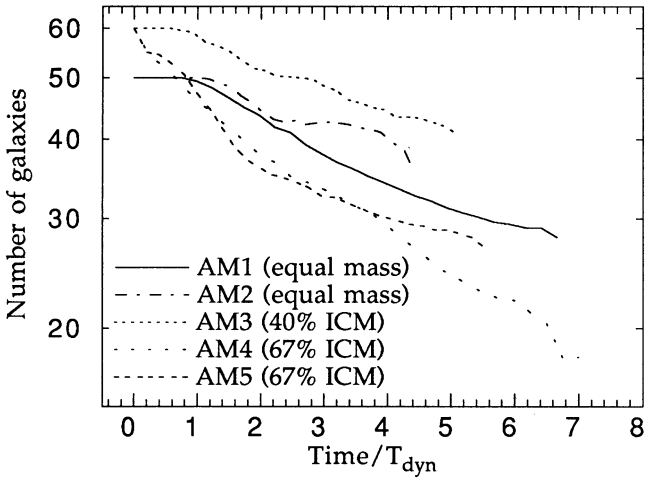

Fig. 4a. Evolution of the number of galaxies (merging rate) for the simulations of isolated clusters. In order to compare, the time scale is normalized by the dynamical time scale (see Tables 2 and 3). The number of galaxies is plotted in logarithm scale to emphasize the exponential character. Note that in some places curves are not strictly decreasing because when 2 or more galaxies are too close together, they are counted as one by the 'friends-of-friends' algorithm. Later, when the galaxies separate, they are counted individually again

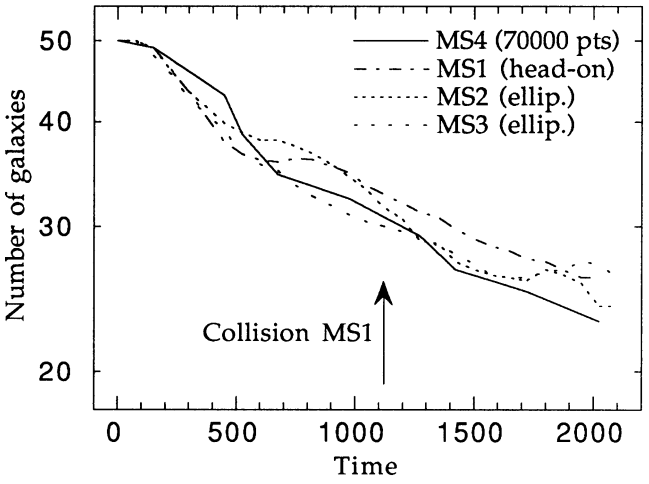

Fig. 4b. The same as Fig. 4a for the simulations of collisions of subclusters. As a reference, it is showed the first collision in simulation MS1. The initial mean dynamical time scale of the subclusters is 400 time units

sive ICM, the mass contained in the galaxies is about the same for both simulations).

For the simulations of merging of substructures, (MS1, MS2, MS3, and MS4) the formation of a dominant galaxy is not different from the simulations AM3 and AM4. Indeed, the merging rate does not seem to change even when the substructures collide. Each substructure develops its own dominant galaxy at its centre. These FRGs, however, will promptly merge when the substructures collide. The time scale of merging of these galaxies is comparable to the time scale of merging of the ICM of both substructures.

Table 6. χ^2-fit of the combined merging rate of the MS simulations (collision of subclusters). 'Prob($>\chi^2$)', the confidence of the fit, gives the probability of having a χ^2 higher than the one we got. The column 'Fit' gives the equations used to fit the merging rate; n_0 is the normalization constant and b is the 'inclination' slope in time units. t is the time

Fit	b	χ^2	Prob($>\chi^2$)
$n_0 - t/b$	84.8	76.7	87.4%
$n_0 \exp(-t/b)$	2750	143.3	1.0%

The decrease of the number of galaxies in all the simulations presented here (Figs. 4a and b) are best represented as an exponential decrease, rather than a linear one. In order to have a quantitative measure, we have combined the number of galaxies as a function of time for the four MS simulations (collision of two subclusters) and made a χ^2-fit to a linear and exponential curve (Table 6).

These fits suggest that the merging rate can be expressed as $\mathrm{d}N_{\mathrm{gal}}/\mathrm{d}t \propto -N_{\mathrm{gal}}$, implying that the number of mergers in a given cluster is proportional to the number of galaxies, being higher in the past than now.

3.2. Mass evolution of the FRG and its envelope

As the galaxies evolve in the cluster, a fraction of their mass is stripped by tidal encounters and forms a diffuse component in the cluster. This diffuse component ends on a huge envelope around the central dominant galaxy (cf. Figs. 1, 2, and 3). Here, we analyse the mass evolution of this stripped matter as well as the mass of the FRG.

Fig. 5 shows the mass growth rate of the FRG and the diffuse component stripped from the galaxies. (The dark ICM particles are not used to compute the mass in the FRG.) Both the envelope and the FRG have a strong increase in mass during the first 1–2 t_{dyn}. The strong evolution of the FRG mass and its envelope corresponds to the higher merging rate observed at the beginning of the simulations. The FRG then basically stops growing but the envelope goes on accreting stripped matter from the galaxies.

The reason why the FRG mass growth almost halts is related to our definition of FRG and envelope. Indeed, what we call the FRG is the central part of the galaxy (cf. Sect. 2.3). Therefore, the FRG mass cannot grow indefinitely. On the other hand, the envelope is formed by the stripped particles from the all the galaxies. Its increase reflects the tidal interactions and mergers in the cluster.

Inspection of Figs. 1, 2, and 3 suggests that the mergers occur mainly with the central dominant galaxy. In order to verify this we plot the combined mass of the FRG (the galaxy plus its envelope) vs. the number of galaxies in the cluster (Fig. 6). Indeed, this plot shows a strong correlation between the growth of the total mass of the FRG and the rate of merging, thus strengthening our suspicion that mergers are mostly related with the central dominant galaxy.

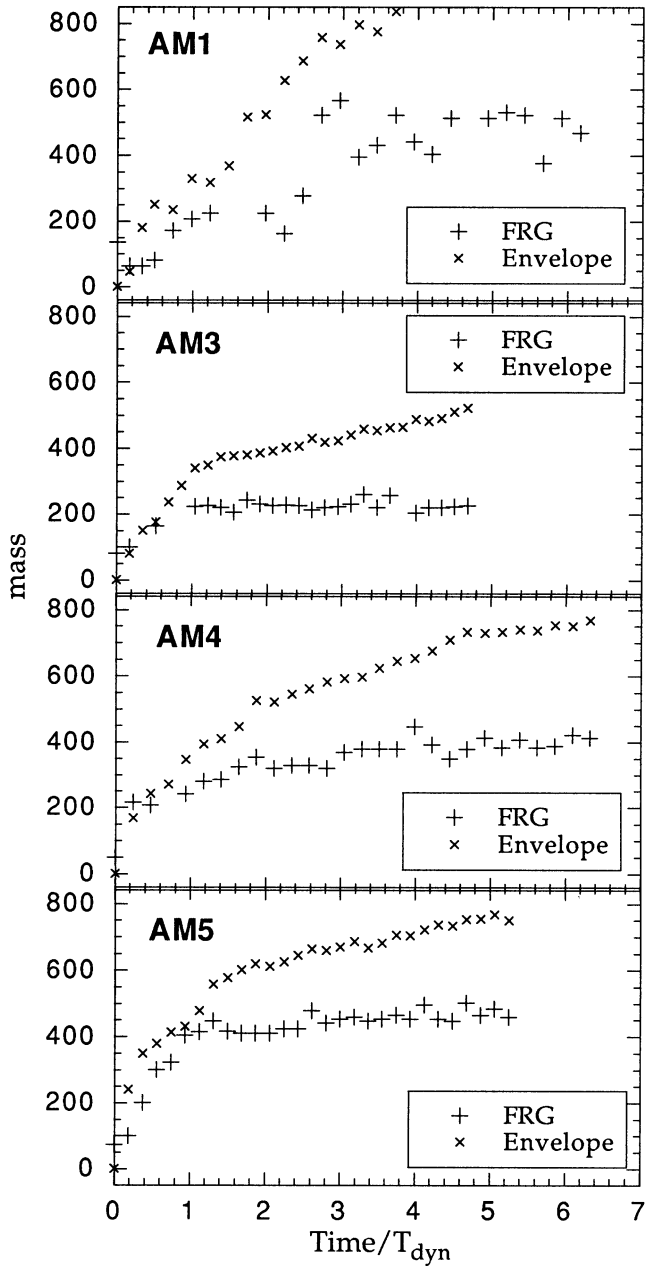

Fig. 5. Mass growth rate of the FRG and its envelope. For comparison purpose, the time is scaled to the dynamical time scale. The run ids. are on the top left of each panel

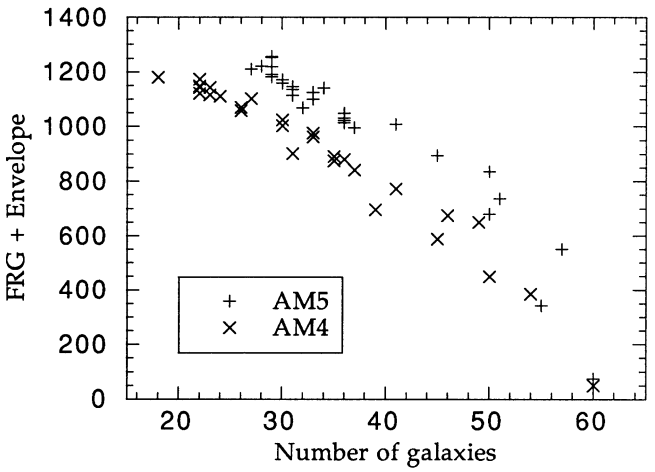

Fig. 6. Total mass of the FRG (galaxy + envelope) as a function of the number of galaxies for two simulations, AM4 and AM5

3.3. Position and velocity of the FRG

As it was seen above, the FRG is always near the centre of the cluster. In Figs. 7a and 7b we show the position of the FRG as a function of time for the simulations of isolated clusters and colliding clusters.

The FRG is not always formed already in the centre. In the simulations AM1 and AM3, the FRGs are formed at more than $\sim$ 200 kpc from the centre of the cluster. In the simulations AM4 and AM5 the FRGs are formed in the core, at about 80 kpc from the centre. The FRGs of simulations AM1 and AM3 falls towards the centre and remain in the core.

In all simulations, the FRGs oscillate around the centre of the cluster. However, the amplitude of this oscillation depends strongly on the amount of ICM. In the simulation AM1, initially without ICM, the amplitude of the oscillation reaches 160 kpc even after 5 $t_{\rm dyn}$ (or 9.6×10^9yr). Increasing the ICM, results in a decreasing oscillation amplitude; the simulation AM3 reaches at most 120 kpc, and the simulations AM4 and AM5, with the highest ICM, have maximum amplitude of $\sim$ 40 kpc.

Likewise, the FRGs velocity decreases with increasing ICM, although in a less dramatic way (Fig 8a). The FRG velocity in simulation AM1 goes from about 150 to 350 km/s and finally remaining at 100 km/s. In the simulations AM3, AM4 and AM5 the FRGs have an initial velocity of about 150–200 km/s that falls to 80 km/s after 2 $t_{\rm dyn}$.

For the simulations MS1 and MS3 we follow one of the FRGs (there is one for each subcluster). The position and velocity are relative to the centre of mass of the whole system (Figs 7b and 8b). In both simulations the FRGs fall to the centre in $\sim 7\times10^9$yr where they merger with the other subcluster FRG. After merging their behaviour is similar to the FRGs from the isolated cluster simulations. The FRGs of simulations MS1 and MS3 remain at a distance of 30 and 70 kpc from the centre respectively, with a peculiar velocity of $\sim$ 70 km/s.

It is interesting to note that when the FRGs of the colliding subclusters are merging they have a higher peculiar velocity. In the simulation MS1 (head-on collision), at 1300 time units the FRGs are almost merged and have a peculiar velocity of 200 km/s. In simulation MS3 (off-centre collision) we observe the same, the FRGs have a velocity of 160 km/s relative to the centre of the cluster just before finishing merging.

The above values are three dimensional. When projecting the cluster on the plan of the sky and taking only the line-of-sight velocity, the FRG will usually appear to be closer to the centre and with a lower peculiar velocity. These results show that the ICM is efficient to produce the dynamical friction on

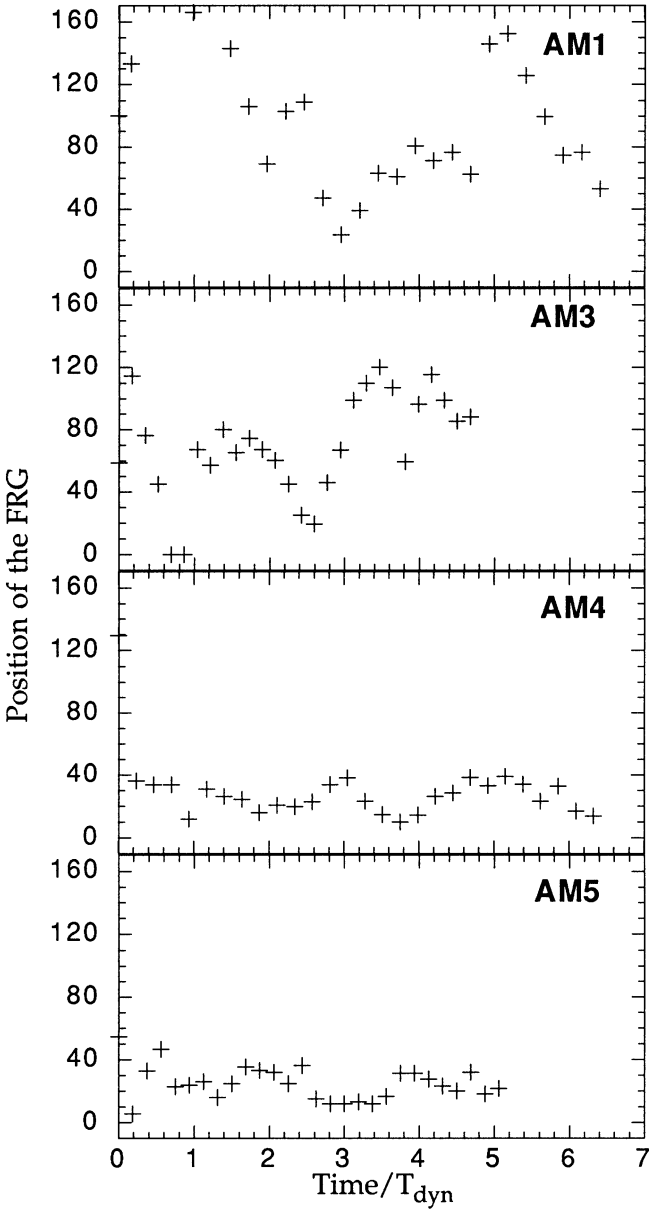

Fig. 7a. Position of the FRG as a function of time for four isolated cluster simulations. For comparison purpose, the time is scaled to the dynamical time scale. The run ids. are on the top right of each panel

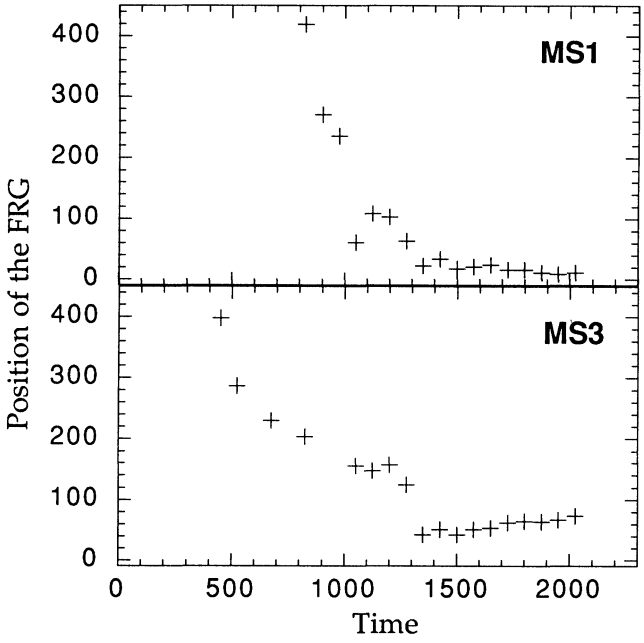

Fig. 7b. Same as Fig. 7a but for the simulations of colliding clusters. The time scale is in our simulations units

the massive galaxies. Notice however that the position is more strongly affected than the velocity of the galaxies.

3.4. The mass function

We have fitted the differential mass function using the Schechter luminosity function at every 75 time-units in order to determine its evolution. Due to the small number of objects in our simulations, the fits were done by maximization of the Likelihood using a Poisson distribution for the probability of having n galaxies in a given interval $M, M + \mathrm{d}M$ where the expected number of galaxies is given by the Schechter distribution. The errors on the fitting parameters are estimated with a Bootstrap (or re-sampling) technique.

The most notable fact observed in our simulations is that there is *no* or very little evolution of the mass function of a cluster. This result applies for isolated clusters as well as for the simulations of merging substructures. There are, however, three factors that must be taken into account before analysing this result. First, the mass range in the simulations is only a factor 12.5 and, second, the number of galaxies varies between 60 to ~ 25 from the beginning to the end of a simulation. Third, as explained in Sect. 2.3, what we identify as a 'galaxy' is actually its central part. More details of the evolution of the mass function are given elsewhere (Lima Neto, 1996).

3.5. Substructures

We have compared the distribution of the galaxy counts with the distribution of the diffuse invisible matter (Figs. 9a and b). The distribution of the ICM (here, the dark collisionless particles) should be similar to an hypothetical emissivity map of X-rays. This is so supposing that the X-ray emitting plasma traces the cluster gravitational potential. Such hypothesis is justified due to the very short relaxation time scale of the X-ray emitting plasma compared to the dynamical time scale of the cluster itself.

In the simulations of isolated clusters with a dark ICM (AM3, AM4 and AM5), the projected isodensity curves are relatively spherically symmetric although rather noisy (Fig. 9b). Small secondary maxima can be seen, always related to a concentration of galaxies. Isopleths of galaxy counts show more structures than the ICM on all simulations, as it seems to be the same case with real clusters (e.g. Baier 1983). Globally, all simulated clusters show some degree of subclustering. This is

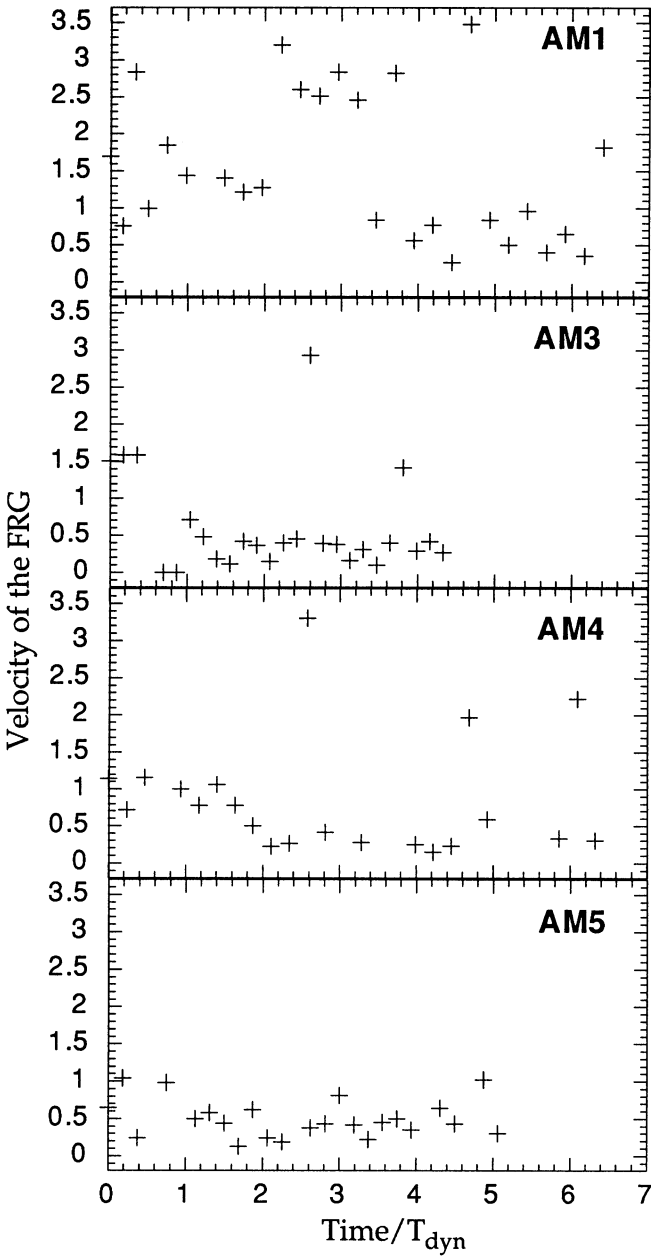

Fig. 8a. Velocity of the FRG as a function of time for four isolated cluster simulations. For comparison purpose, the time is scaled to the dynamical time scale

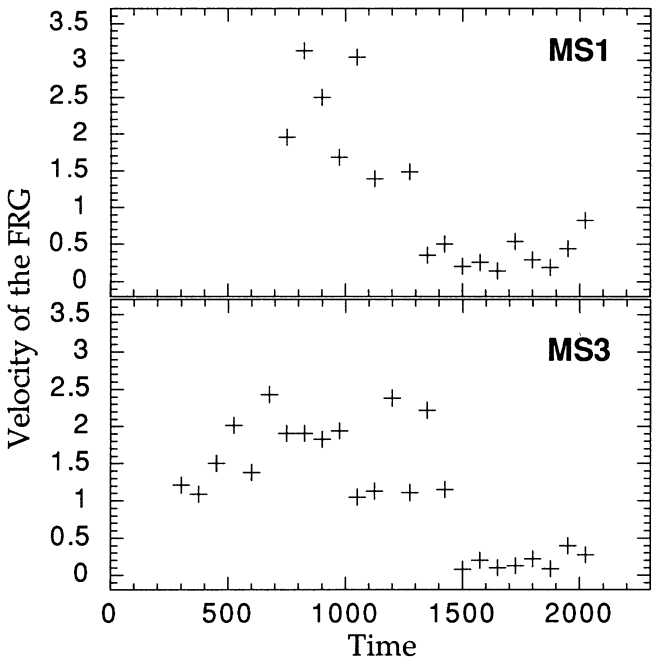

Fig. 8b. Same as Fig. 8a but for the simulations of colliding clusters. The time scale is in our simulations units

of course higher when we have two substructures colliding but the subclustering is nevertheless visible even in the simulations of isolated clusters.

An interesting fact is that in some projections of the clusters the FRG does not coincide with the maximum of the ICM density. For instance, in one case we have the second more massive galaxy at about 50 kpc from centre of the projected ICM distribution and the FRG at about 200 kpc. This happens at a time (in physical units) of 11.8×10^9 years, counting from the beginning of the simulation. Looking at the evolution of this particular simulation, we notice that what happens is that the galaxy closest to the centre was the FRG while the second ranked galaxy was farther away. However, the later merges with another large galaxy at $T \approx 11.0 \times 10^9$ years, and becomes the FRG. Therefore, the offset between the centre of the ICM and the FRG is, in this case, a transient effect which lasts a little less than 10^9 years, the time it took for the FRG falls to the centre of the cluster.

3.6. Rotation in clusters of galaxies

When two gravitationally bound subclusters collide with a non zero impact parameter, the whole system may have a significant amount of angular momentum. The question is if a global rotation of the clusters can be detected. Fig. 10 shows the plot of the galaxy line-of-sight velocity as a function of the position inside the cluster for the simulation MS3.

Given optimal conditions, i.e. the observer being located near the orbital plane of the subclusters and observing them as their projected separation is about the size of their diameter (when the subclusters are just 'touching' each other), one can clearly detect the rotation of the whole cluster around its geometric centre. However, after the two subclusters merge completely, the rotation is less detectable but still present. The angular momentum of the galaxies relative to the centre of the cluster is transferred to the massive ICM. That is similar to what happens with two spiral galaxies of about the same mass that merge and form an elliptical galaxy. The angular momentum of the discs and the orbital angular momentum are transported to the massive halo (Barnes, 1988).

We computed the dimensionless spin-parameter defined by

$$\lambda = G^{-1} J (|E| M^{-5})^{1/2} , \qquad (3)$$

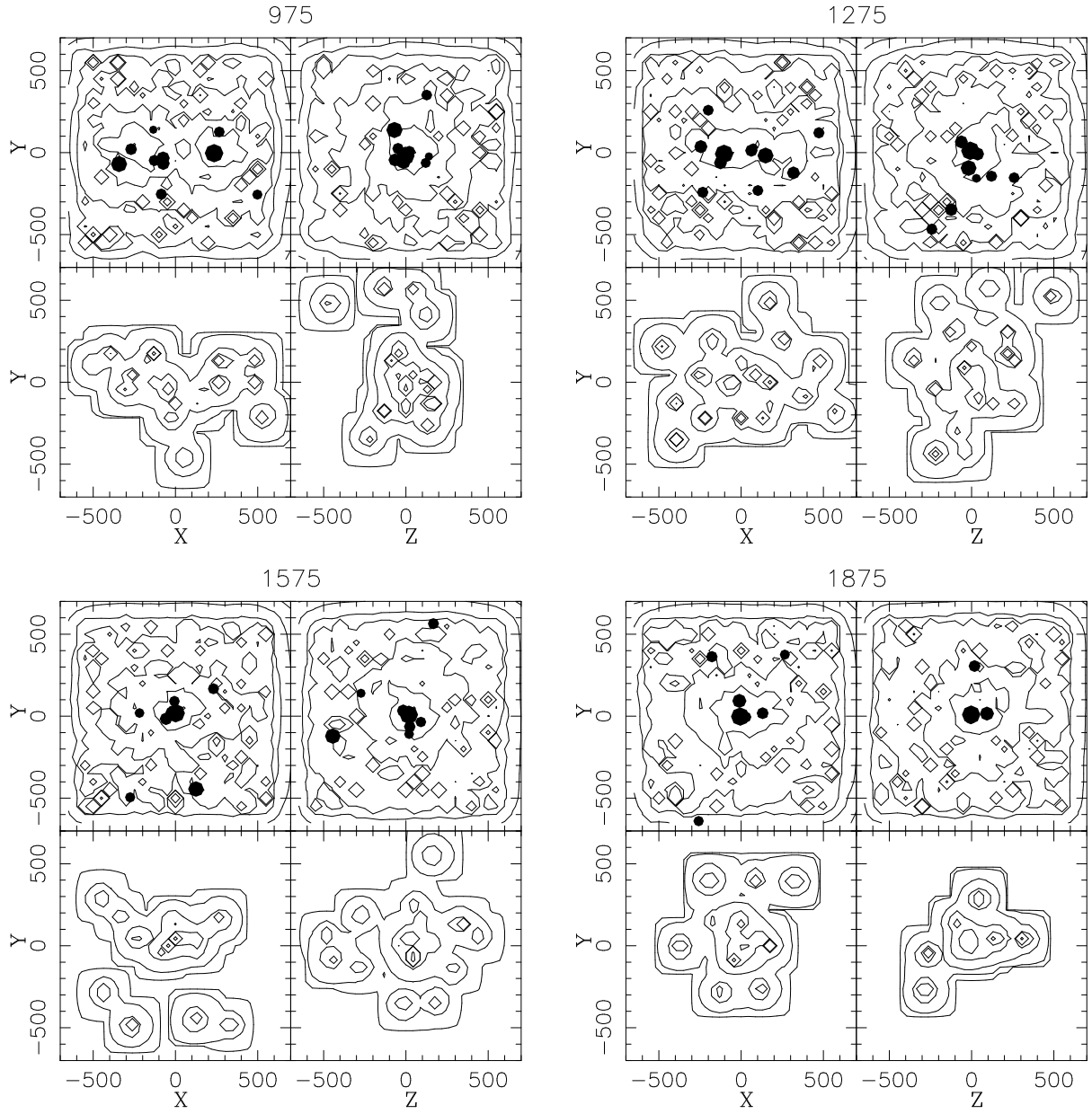

Fig. 9a. Projected isodensities of the ICM compared to the distribution of galaxies of simulation MS1. The upper two panels are two orthogonal projections of the ICM, below are the corresponding isopleths of galaxy counts. The dots superposed to the ICM isocontours represent the most massive galaxies. Above each picture is the time.

where J, E and M are the total angular momentum, energy and mass, respectively. The isolated and the head-on collision simulations have $\lambda \approx 0.02$–0.06. It is not zero due to the random fluctuation when generating the initial conditions that produces some trifling rotation. On the other hand, the simulations of subcluster collision that are initially in an elliptical orbit, specially MS3 and MS4, have $\lambda \approx 0.3$, while the simulation MS2 has $\lambda \approx 0.5$. These values are high in comparison to the predicted rotation of clusters produced only by tidal torques which is about $\lesssim 0.2$ (Efstathiou & Barnes 1984). As a reference, a spiral galaxy has $\lambda \approx 1$.

4. Discussion

A number of N-body simulations of poor clusters of galaxies using particle methods, has been performed by diverse authors recently. Our models relate closely to the simulations of Barnes (1989), Malumuth (1992), Funato et al. (1993), and Bode et al. (1993, 1994).

Similarly to Funato et al. (1993), the stripping of particles that were initially bound to the galaxies is very important. In our simulations, more than half of the particles initially in the galaxies are, at the end of the run (or $\sim 12 \times 10^9$ yr), on a huge envelope around the central dominant galaxy. That means that

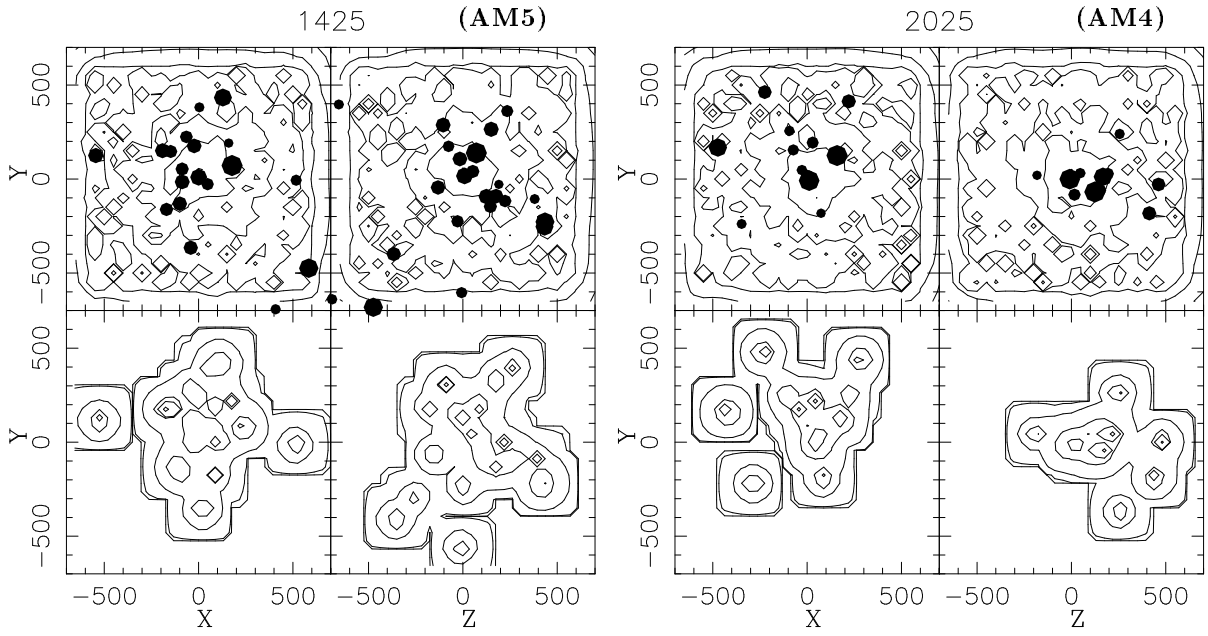

Fig. 9b. Same as Fig. 9a but for simulations AM5 and AM4.

starting with an ICM ($M_{\rm ICM}/M_{\rm tot}$) of 67% we arrive at an ICM of 83% by the end of the simulation.

Contrary to the results of Bode et al. (1994), the number of mergers in our simulations increases with increasing initial ICM. That probably comes from the way the clusters are constructed. When Bode et al. increase their ICM (noted β in their paper) they actually reduce the mass in the galaxies and, consequently, the radius thus reducing the merging cross section of the galaxies. On the other hand, in the simulations here we keep the mass and radius of the galaxies, augmenting the ICM mass and hence the velocity dispersion. The overall effect is to increase the dynamical friction which facilitates the formation of the central dominant galaxy by cannibalism. The merging rate is thus higher because mergers occur mainly with the central cannibal galaxy.

The collision of subclusters has been intensely investigated with the help of numerical simulations during the last few years (e.g. Roettiger et al. 1993, Jing et al. 1995, and Nakamura et al. 1995). The simulations of Roettiger et al. (1993) are based on a hybrid hydrodynamics–tree-code appropriate to follow the X-ray emitting gas but lacking enough particles to resolve the galaxies. Jing et al. (1995) P^3M simulations have pertinent cosmological initial conditions but again do not resolve the individual galaxies.

Nakamura et al. (1995) use direct summation to solve the equations of motion and, also, do not resolve the galaxies. They conclude from their experiments that the initial distribution of the invisible matter is relevant to determine the time scale for erasing the substructure feature after the collision of the substructures. They estimate that this can take more than 4×10^9yr after the first encounter. In our simulation MS1 (head-on collision of subclusters) it takes about 2.6×10^9yr after the first encounter for the substructures of the mass distribution to be erased. This difference seems to be simply due to the slightly lower relative velocity between the subclusters that we adopted, 1.5 instead of 1.92 that we would have using their prescription (based on having the clusters at rest at infinity). In other words, our simulation has a higher binding energy and the double peak is washed out faster.

Malumuth (1992) simulated clusters of 100 galaxies with 50% of the mass in the ICM using an 'explicit physics' code (i.e. dynamical friction, merging, and tidal stripping are treated in a statistical way) in order to study the peculiar velocities of cD galaxies. The position and velocity of the FRGs in our simulations are in agreement with his work, where 78% of his cD galaxies lie closer than 100 kpc from the centre and 72% have a velocity lower the 150 km/s. Malumuth also suggested that cD galaxies with high peculiar velocity should be found preferentially in clusters with substructures. Indeed, in our simulations the FRGs with higher peculiar velocity are found in colliding clusters (where substructures are most significant) at the moment that the subclusters are merging. However, after the FRGs from both subclusters merge and form a single giant galaxy, it quickly falls to the centre and is braked there by dynamical friction. Thus, a cD galaxy could be detected with a high peculiar velocity during an interval of ~ 1–3×10^9yr, taking into account the time it takes for the merging and braking by dynamical friction.

Although the distribution of galaxies is clumpier than the ICM, the galaxy distribution reflects the total matter distribution. Thus, if the intra-cluster plasma traces the gravitational potential, the galaxy distribution should trace the X-ray emission. This seems to be indeed the case in real poor clusters (Dell'Antonio et al 1995).

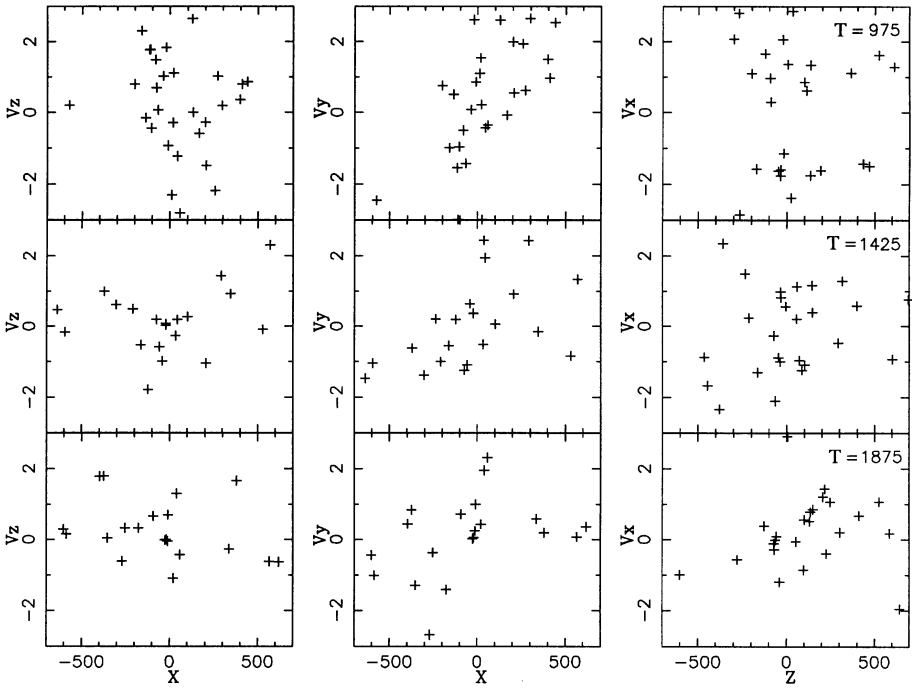

Fig. 10. Line-of-sight velocity as a function of the projected distance from the centre of the cluster for the simulation MS3. Each column represents a perpendicular projection of the cluster. The time is shown on the panels on the right column. A rotational pattern can be seen when the cluster is observed from near the orbital plane (Y–Z)

The collision and merger of two subclusters initially in a highly elliptical orbit produces a final cluster with an amount of rotation detectable with the line-of-sight velocity of the galaxies. Although the observer must be close to the orbital plane of the subclusters, the analysis of clusters classified as elongated, flattened or bi-modal may show a rotational pattern of the galaxies around the centre of the cluster. Since tidal torques are not enough to produce the rotation on this scale (Efstathiou & Barnes, 1984), the observation of rotating clusters would support hierarchical cosmological theories where smaller units merge to form bigger ones. At least one cluster, SC 0316-44, has a velocity pattern that corresponds closely to our simulation MS3 (Materne & Hopp 1983). It is an elongated cluster containing two massive galaxies, a cD and a D. This may be a case of two subclusters spiraling towards each other.

It is interesting to note that the collision of substructures does not seem to affect the rate that galaxies merge. As stated above, mergers occur preferably with the central cannibal galaxy rather than pairwise (as already noted by Bode et al. 1994). Since the cannibal galaxy formation is faster than the coalescence of substructures, it is natural to understand the small (or none) effect of subcluster collisions on the merging rate of galaxies. Thus, each substructure behaves as an isolated mini cluster, forming its own FRG and cannibalizing the smaller ones almost independently of its surroundings.

At last, increasing the number of particles from 46 000 to 70 000 shows no effect on the evolution of our simulations.

5. Conclusion

We have performed N-body simulations of poor clusters using enough particles to model the internal structure of the galaxies in a self-consistent way. The main results of this work are resumed as follows.

The merging of substructures does *not* increases the merging rate of galaxies in clusters of galaxies. However, it seems to be an efficient mechanism to produce cD galaxies near the centre of the potential wells, where the ICM and the cD galaxy of each substructure have merged. Moreover, the growth rate of the FRG is strongly correlated with the merging rate in a cluster.

The position of the first ranked galaxy does *not* coincide always with the maximum density of the dark matter, even in an isolated cluster. Assuming that the intra-cluster X-ray emitting gas traces the gravitational potential of a cluster (dominated by the invisible matter) this implies that the position of the FRG may not match the maximum X-ray emission of a cluster.

The merger of substructures (or merger of poor clusters) may produce situations where the position of the FRG does not coincide with the position of the deepest point of the potential well produced by the dark matter. This offset is most visible just after the merging of the dominant galaxies of each substructure. This situation can also be observed in isolated clusters, when the dominant galaxy is still oscillating around the centre of the cluster.

Our simulations suggest that the initial mass function of the galaxies is narrowly related to the formation and development of an important central FRG with cD characteristics. A steep mass distribution function facilitates the creation of a central dominant galaxy whereas a flat distribution tends to slow its formation.

The shape of the mass distribution function shows no or only a very small evolution during the life span of a cluster, even when there are pronounced substructures. This result, however, should

be regarded carefully since the mass range in these simulations was small (~ 12) compared to a real cluster of galaxies.

Finally, the merger of two subclusters with a non zero impact parameter can produce a detectable (with the observation of the line-of-sight velocity), rotating cluster of galaxies.

Acknowledgements. One of us (G.B.L.N.) thanks the support from the Alexander von Humboldt Foundation. The computations were performed on the Crays J90 and EL92 of the *Astrophysikalisches Institut Potsdam*.

References

Albert, C.E., White R.A., Morgan W.W., 1977, ApJ 211, 309
Baier F.W., 1983, Astron. Nachr. 304, 211
Baier F.W., Lima Neto, G.B., Wipper H., Braum M., 1996, Astron. Nachr. 317, 77
Bahcall N.A., 1980, ApJ Lett. 238, L117
Barnes J., 1988, ApJ 331, 699
Barnes J., 1989, Nature 338, 123
Barnes J., Hut P., 1986, Nature 324, 446
Beers T.C., Forman W., Huchra J.P., Jones C., Gebhardt K., 1991, Astron. J. 102, 1581
Bode P.W., Cohn H., Lugger P., 1993, ApJ 416, 17
Bode P.W., Berrington R.C., Cohn H.N., Lugger P.M., 1994, ApJ 433, 479
Chincarini G., Vettolani G., de Souza R.E., 1988, A&A 193, 47
Dell'Antonio I.P., geller M.J., Fabricant D.G., 1995, AJ 110, 502
Efstathiou G., Barnes J., 1984, in: Formation and evolution of galaxies and large structures in the Universe, p. 361, Audouze J. and Tran Thanh Van J. eds., D. Reidel Publishing Company
Fabian A.C., Nulsen P.E.J., Canizares C.R., 1984, Nature 310, 30
Fort B., Mellier Y., 1994, A&AR 5, 239
Funato Y., Makino J., Ebisuzaki T., 1993, PASP 45, 289
Geller M.J., Beers U.G., 1982, PASP 94, 421
Hernquist L., 1988, Comp. Phys. Comm. 48, 107
Lima Neto G.B., 1996, Astr. Letts. Comm., submited
Jing Y.P., Mo H.J., Börner G., Fang L.Z., 1995, MNRAS 276, 417
Jones C., Forman W., 1990, in: Clusters of Galaxies, p. 257, Oegerle W.R., Fitchett M.J. and Danly L. editors, Cambridge Univ. Press
Malumuth E. M., 1992, ApJ 386, 420
Materne J., Hopp U., 1983, A&A Lett. 124, L13
McGlynn T.A., Fabian A.C., 1984, MNRAS 208, 709
Merritt D., 1983, ApJ 264, 24
Morgan W.W., Kayser S., White R.A., 1975, ApJ 199, 545
Nakamura F.E., Hattori M., Mineshige S., 1995, A&A 302, 649
Ostriker J.P., Tremaine S.D., 1975, ApJ Lett. 202, L113
Roettiger K., Burns J., Loken C., 1993, ApJ Lett. 407, L53
Sarazin C.L., 1988, "X-ray emissions from clusters of galaxies", Cambridge University Press
Schechter P., 1976, ApJ 203, 297
Ulmer M.P., Wirth G.D., Kowalski M.P., 1992, ApJ 397, 430
West M.J., Oemler A., Dekel A., 1988, ApJ 327, 1
Zabluboff A.I., Zaritsky D., 1995, ApJ Lett. 447, L21

This article was processed by the author using Springer-Verlag LaTeX A&A style file *L-AA* version 3.